

Comparison of $\delta^{13}\text{C}$ analyses of individual foraminifer (*Orbulina universa*) shells by secondary ion mass spectrometry and gas source mass spectrometry

Jody B. Wycech^{1,2}  | Daniel Clay Kelly²  | Reinhard Kozdon^{2,3}  |
 Akizumi Ishida²  | Kouki Kitajima²  | Howard J. Spero⁴  | John W. Valley² 

¹US Geological Survey, Central Energy Resources Science Center, Denver, Colorado, USA

²Department of Geoscience, University of Wisconsin-Madison, Madison, Wisconsin, USA

³Lamont-Doherty Earth Observatory of Columbia University, Palisades, New York, USA

⁴Department of Earth & Planetary Sciences, University of California Davis, Davis, California, USA

Correspondence

J. Wycech, US Geological Survey, Central Energy Resources Science Center, Denver, CO 80225, USA.

Email: jwycech@usgs.gov

Present address

Akizumi Ishida, Graduate School of Science Department of Earth Science, Tohoku University, Sendai, Miyagi, Japan.

Funding information

National Science Foundation, Grant/Award Numbers: EAR-1658823, EAR-2004618, OCE-0550703, OCE-1405224; U.S. Department of Energy (Office of Science, Office of Basic Energy Sciences and Energy Efficiency and Renewable Energy, Solar Energy Technology Program), Grant/Award Number: DE-FG02-93ER14389

Abstract

Rationale: The use of secondary ion mass spectrometry (SIMS) to perform micrometer-scale *in situ* carbon isotope ($\delta^{13}\text{C}$) analyses of shells of marine microfossils called planktic foraminifers holds promise to explore calcification and ecological processes. The potential of this technique, however, cannot be realized without comparison to traditional whole-shell $\delta^{13}\text{C}$ values measured by gas source mass spectrometry (GSMS).

Methods: Paired SIMS and GSMS $\delta^{13}\text{C}$ values measured from final chamber fragments of the same shell of the planktic foraminifer *Orbulina universa* are compared. The SIMS–GSMS $\delta^{13}\text{C}$ differences ($\Delta^{13}\text{C}_{\text{SIMS-GSMS}}$) were determined via paired analysis of hydrogen peroxide-cleaned fragments of modern cultured specimens and of fossil specimens from deep-sea sediments that were either untreated, sonicated, and cleaned with hydrogen peroxide or vacuum roasted. After treatment, fragments were analyzed by a CAMECA IMS 1280 SIMS instrument and either a ThermoScientific MAT-253 or a Fisons Optima isotope ratio mass spectrometer (GSMS).

Results: Paired analyses of cleaned fragments of cultured specimens ($n = 7$) yield no SIMS–GSMS $\delta^{13}\text{C}$ difference. However, paired analyses of untreated ($n = 18$) and cleaned ($n = 12$) fragments of fossil shells yield average $\Delta^{13}\text{C}_{\text{SIMS-GSMS}}$ values of 0.8‰ and 0.6‰ ($\pm 0.2\text{‰}$, 2 SE), respectively, while vacuum roasting of fossil shell fragments ($n = 11$) removes the SIMS–GSMS $\delta^{13}\text{C}$ difference.

Conclusions: The noted $\Delta^{13}\text{C}_{\text{SIMS-GSMS}}$ values are most likely due to matrix effects causing sample–standard mismatch for SIMS analyses but may also be a combination of other factors such as SIMS measurement of chemically bound water. The volume of material analyzed via SIMS is $\sim 10^5$ times smaller than that analyzed by GSMS; hence, the extent to which these $\Delta^{13}\text{C}_{\text{SIMS-GSMS}}$ values represent differences in analyte or instrument factors remains unclear.

This is an open access article under the terms of the [Creative Commons Attribution-NonCommercial-NoDerivs](#) License, which permits use and distribution in any medium, provided the original work is properly cited, the use is non-commercial and no modifications or adaptations are made.

© 2023 The Authors. *Rapid Communications in Mass Spectrometry* published by John Wiley & Sons Ltd. This article has been contributed to by U.S. Government employees and their work is in the public domain in the USA.

1 | INTRODUCTION

Carbon isotope ratios (expressed as $\delta^{13}\text{C}$) measured from the biogenic calcite (CaCO_3) of microscopic shells grown by foraminifera, a group of marine protists that have an extensive fossil record, are a commonly used geochemical proxy for reconstructing past ocean carbon chemistry. Foraminifer $\delta^{13}\text{C}$ values are used to constrain past patterns and rates of ocean overturning,^{1,2} water column hydrography,³ paleo-productivity,^{4,5} and past perturbations to the global carbon cycle.^{6,7} However, such reconstructions of ocean-climate history require the use of foraminifer shells that have retained their original $\delta^{13}\text{C}$ composition over time. Well-preserved material in the deep-sea sedimentary archive is often mixed together with fossil foraminifer shells that have been altered through carbonate dissolution, chemical exchange with sedimentary pore fluids, and/or the addition of diagenetic cements.^{8–10} Furthermore, intrashell $\delta^{13}\text{C}$ variability could occur due to the complex life histories and ecologies of some planktic foraminifer species. For instance, shell formation in a water column with a steep thermal gradient or variably sourced food supply could lead to intrashell $\delta^{13}\text{C}$ variability during calcification.^{11,12} Furthermore, many planktic foraminifer species host algal symbionts whose photosynthetic activity increases both the whole-shell $\delta^{13}\text{C}$ value and intrashell $\delta^{13}\text{C}$ variability due to day-to-night changes in calcification.^{11,13,14} Many “mixed layer” species inhabiting the warm, sunlit waters of the photic zone also sink to deeper waters during their terminal ontogenetic stage of reproduction (gametogenesis) where a crust of calcite is rapidly added to the outer surface of their shell.^{15–17} Information about this intrashell $\delta^{13}\text{C}$ heterogeneity is lost when using conventional gas source mass spectrometry (GSMS) because such analyses require acid digestion and isotope ratio measurements of whole shells that would be aggregate mixtures of CaCO_3 that precipitated under differing environmental and physiological conditions.¹⁸

The SIMS laboratory in the Department of Geoscience at the University of Wisconsin-Madison (WiscSIMS) has developed analytical techniques and procedures to address the loss of geochemical heterogeneity information by conventional GSMS $\delta^{13}\text{C}$ analyses. To this end, secondary ion mass spectrometry (SIMS) is now being used to acquire *in situ* $\delta^{13}\text{C}$ measurements on micrometer-scale domains within biogenic carbonate minerals, including individual foraminifer shells.^{19–22} The ultrahigh spatial resolution (1–7 μm) of SIMS $\delta^{13}\text{C}$ analysis permits isolated measurement in a desired domain of an individual shell. This *in situ* technique has been used to quantify the effects of diagenesis on the $\delta^{13}\text{C}$ of fossil planktic foraminifer shells^{19,23} and to delineate intrashell $\delta^{13}\text{C}$ variation that reflects experimentally induced geochemical bands in cultured planktic foraminifers.²¹

The study described herein is the first to compare SIMS and GSMS $\delta^{13}\text{C}$ values from the same foraminifer chamber to assess possible SIMS-GSMS differences and better understand the paleoenvironmental signals measured by the two techniques. This interinstrument $\delta^{13}\text{C}$ comparison was conducted using the extant, mixed-layer dwelling planktic foraminifer *Orbulina universa*. This

particular species was selected for three reasons: (1) field and culturing studies have established the ecological affinities of this symbiont-bearing, mixed-layer foraminifer^{24,25}; (2) shell $\delta^{13}\text{C}$ in *O. universa* calcite has been empirically calibrated against the carbon isotope composition of dissolved inorganic carbon ($\delta^{13}\text{C}_{\text{DIC}}$)^{11,13,26,27}; and (3) this species grows a large spherical chamber at the end of its lifecycle that incorporates <10 days of chamber calcification.^{28,29} The latter attribute is particularly advantageous because the final spherical chamber is massive (25–100 $\mu\text{g}/\text{shell}$), displays consistent geochemistry around its circumference,³⁰ and can be broken into fragments for analysis without contamination from the juvenile chambers found in the earlier trochospiral part of the same shell. Thus, we can quantify the SIMS-GSMS $\delta^{13}\text{C}$ difference ($\Delta^{13}\text{C}_{\text{SIMS-GSMS}}$) through analysis of identical foraminifer material using these two measurement techniques.

2 | METHODS

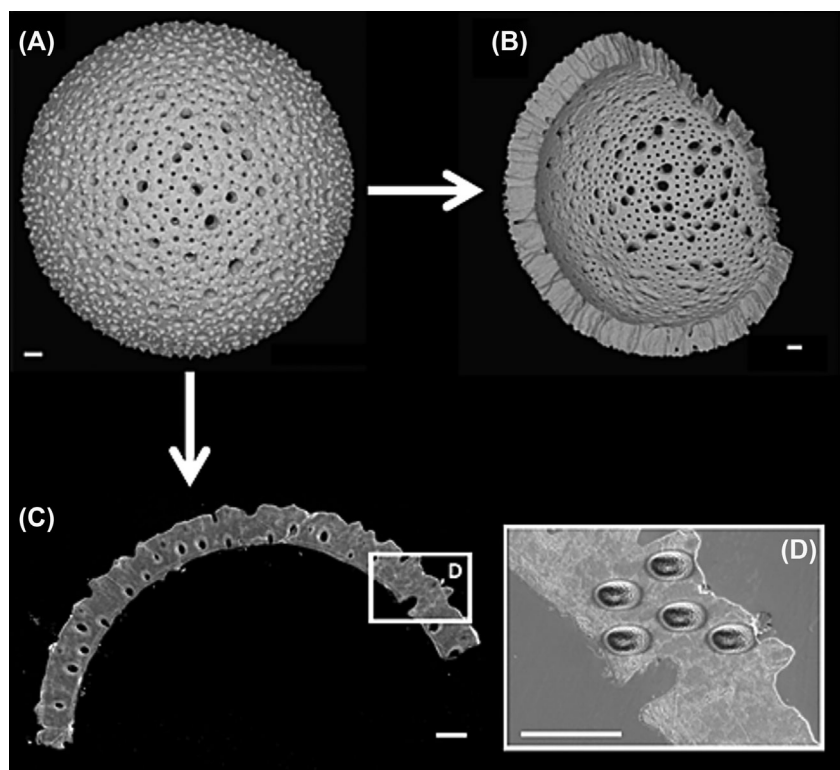
2.1 | Cultured shells grown under controlled conditions

Paired SIMS-GSMS $\delta^{13}\text{C}$ analyses were performed on seven *O. universa* shells grown in the laboratory. These shells were cultured in 1995 as part of a larger experiment described by Bemis et al (Table A1).³¹ Specimens were maintained at constant temperature ($22 \pm 0.2^\circ\text{C}$), $\delta^{13}\text{C}_{\text{DIC}} = 1.3\text{‰}$, salinity = 33.3‰, pH = 8.04, and with an ambient $[\text{CO}_3^{2-}]$ (2250 $\mu\text{mol kg}^{-1}$). Four of the specimens were grown under a 12 h light:12 h dark cycle, one of which was under low light intensity (26–30 $\mu\text{mol photons m}^{-2} \text{s}^{-1}$) and the other three were under high light intensity (400–700 $\mu\text{mol photons m}^{-2} \text{s}^{-1}$). An additional three specimens were grown under continuous 24 h low light intensity. The final chambers of these cultured *O. universa* specimens calcified over a period of 3–9 days. Each shell was manually broken into fragments with a surgical scalpel blade.²¹ Whenever present, juvenile chambers were removed and one or two of the final chamber fragments were used for *in situ* $\delta^{13}\text{C}$ analyses by SIMS and the remaining fragments of the same final chamber were pooled for $\delta^{13}\text{C}$ analysis by GSMS (Figure 1). Sample weights of pooled chamber fragments used for the GSMS analyses ranged from 10 to 90 μg . This “paired” approach permits direct comparison of SIMS and GSMS $\delta^{13}\text{C}$ values obtained from the same spherical, final chamber of each *O. universa* shell.

2.2 | Core-top specimens

Fossil shells of *O. universa* were handpicked from the uppermost 3 cm of piston core CH15-PC9-00 (PC9) collected atop Blake Ridge (2790 m water depth; $31^\circ 55.691'\text{N}$, $75^\circ 43.774'\text{W}$) in the northwestern Atlantic (Figure A1). Radiocarbon dating of the Site PC9 core-top sample has confirmed its Holocene age.³² The sample was

FIGURE 1 SEM images depicting chamber fragmentation method used in this study. All scale bars are 20 μm . (A) BSE SEM image of intact *Orbulina universa* shell taken from the core-top of PC9. (B) BSE SEM image of final chamber fragment (Shell E25) used for GSMS analysis. (C) SE SEM image of remaining fragment (shell CAL1-13) cast in epoxy and cross-sectioned for SIMS analysis. (D) Magnified SE SEM image of area noted in (C) showing SIMS $\delta^{13}\text{C}$ pits across the shell wall.



disaggregated in a mild pH-buffered solution made of sodium hexametaphosphate, hydrogen peroxide (30% v/v), and distilled water, then rinsed with tap water over a 63 μm sieve. The resulting coarse fraction ($>63\ \mu\text{m}$) was subsequently rinsed with distilled water before being oven-dried (30°C) overnight. The *O. universa* shells were handpicked from the $>355\ \mu\text{m}$ sieve-size fraction. The surface texture of each *O. universa* shell was examined using back-scattered electron (BSE) imaging with a Hitachi S-3400N scanning electron microscope (SEM) in variable pressure mode (Dataset S1). The final chamber of each specimen was manually broken into fragments, further treated based on their experimental group (see next paragraph), and then analyzed by GSMS and SIMS.

Three experiments were carried out on the *O. universa* shells extracted from the PC9 sample to compare complementary SIMS and GSMS $\delta^{13}\text{C}$ values. Shell fragments analyzed by SIMS and GSMS in each experiment were pretreated in the same manner prior to final analytical preparation. In the first experiment on untreated shells, final chambers were not cleaned or treated beyond picking the shells from the sample, cracking them open, and analyzing the calcite fragments. In the second experiment, the chamber fragments (not powdered) were cleaned with hydrogen peroxide to remove organic matter and sonicated in methanol to remove material adhering to the surface of the fragments.²¹ The third experiment entailed splitting the final chamber of each shell into three fragments; one fragment was analyzed by GSMS without treatment, while the second and third fragments were roasted *in vacuo* at 375°C for 30 min to remove labile organic carbon and water. One of the vacuum-roasted fragments was analyzed by GSMS and the other vacuum-roasted fragment was analyzed by SIMS.

2.3 | *In situ* $\delta^{13}\text{C}$ measurement by SIMS

The *O. universa* chamber fragments and three grains of the UWC-3 calcite standard ($\delta^{13}\text{C} = -0.9\text{‰}$ scaled to Vienna Pee Dee Belemnite, VPDB)³³ were placed within a 10 mm diameter circular area, cast in a 25 mm diameter epoxy mount, ground to the level of best exposure in cross-section, polished with a carbonate-epoxy relief of less than $\sim 1\ \mu\text{m}$,³⁴ and gold coated. Secondary electron (SE) SEM images (Dataset S2) were taken of each mounted shell fragment in high-vacuum mode to assess the quality of sample exposure and cross-section geometry prior to SIMS analysis.

In situ $\delta^{13}\text{C}$ analyses were performed with a CAMECA IMS 1280 ion microprobe (SIMS) at the WiscSIMS laboratory using a $^{133}\text{Cs}^+$ primary ion beam with an intensity of 300 pA. Each series of 8–12 measurements of foraminifer calcite $\delta^{13}\text{C}$ was bracketed by 4–6 consecutive $\delta^{13}\text{C}$ analyses (before and after) of a UWC-3 standard grain that was cast in the center of the sample mount. The bracketing analyses of UWC-3 were used to determine calcite instrumental mass fractionation (IMF) corrections for each set of foraminifer measurements. After analysis, each SIMS pit was individually imaged (Dataset S3) and examined by SEM using the SE detector in high-vacuum mode (see Figure A2). SIMS pits intersecting cracks and/or epoxy were omitted. Raw and final processed data are reported in standard per mil (‰) notation versus the VPDB standard (Tables S1 and S2).

The 7 μm SIMS pits were measured with a primary beam intensity of 300 pA using instrument settings and an analytical approach comparable to that of Vetter et al.²¹ The resulting secondary $^{12}\text{C}^-$, $^{13}\text{C}^-$, and $^{13}\text{CH}^-$ ions were simultaneously detected

using a Faraday cup ($^{12}\text{C}^-$) and two electron multipliers ($^{13}\text{C}^-$, $^{13}\text{CH}^-$) with a typical $^{12}\text{C}^-$ count rate of 5.0×10^6 counts per second (cps). Simultaneous measurement of $^{13}\text{CH}^-$ with $^{12}\text{C}^-$ and $^{13}\text{C}^-$ during SIMS analysis provides $^{13}\text{CH}^-/\text{CH}^-$ ratios (CH/C hereafter), which are used to gauge the hydrogen content in the sample, likely in the form of organic matter, water, or hydrated CH-bearing phases. The analytical compartment within the SIMS, outgassing of the epoxy mount, and the sample surface contribute to a small background signal even at high vacuum, so the reported CH/C ratios were background-corrected by subtracting the average CH/C of the UWC-3 bracketing data from the CH/C ratio of the foraminifer. UWC-3 is a high-temperature metamorphic calcite and assumed to be anhydrous. In addition to pit appearance, the CH/C ratio and $^{12}\text{C}^-$ count rate served as a basis for assessing the quality of each intervening sample measurement (see Appendix A). The electron multiplier gain was monitored before the third analysis of each group of UWC-3 standard analyses and, when necessary, the high voltage applied to the detector was increased by 2–7 V to compensate for drift in the electron multiplier gain. The total analytical time per analysis was 4 min comprising pre-sputtering (20 s), automatic centering of secondary ions in the field aperture (~ 60 s), and 20 analytical cycles (8 s each). The reproducibility of $\delta^{13}\text{C}$ values of individual analyses on the UWC-3 calcite standard grain bracketing the samples ranged from 0.4‰ to 1.3‰ (2 SD) (average = 0.8‰) and is assigned as the uncertainty range of individual sample measurements. A total of 326 SIMS measurements were performed on *O. universa* chambers (Table S1) in addition to 165 bracketing measurements of the UWC-3 standard.

2.4 | $\delta^{13}\text{C}$ measurement by GSMS

The $\delta^{13}\text{C}$ compositions of chamber fragments from cultured *O. universa* shells, as well as vacuum-roasted chamber fragments of *O. universa* shells from the PC9 core-top, were measured at the University of California, Davis (UCD) using a Fisons Optima dual-inlet isotope ratio mass spectrometer fitted with a common acid bath auto-carbonate device. The chamber fragments were digested in concentrated orthophosphoric acid (specific gravity = 1.92 g/cm³) at 90°C and corrected for acid-digestion fractionation by paired measurement with a Carrara marble standard ($\delta^{13}\text{C} = 2.1\text{‰}$, VPDB) that was previously calibrated against NBS-19. External analytical precision for $\delta^{13}\text{C}$ measurements on samples of *O. universa* final chamber fragments is $\pm 0.08\text{‰}$ (2 SD).

Untreated and cleaned chamber fragments of *O. universa* shells from the PC9 core-top sample were analyzed at the University of California, Santa Cruz (UCSC) using a ThermoScientific Kiel IV carbonate device interfaced to a ThermoScientific MAT-253 dual-inlet isotope ratio mass spectrometer. The chamber fragments were digested in concentrated orthophosphoric acid (specific gravity = 1.92 g/cm³) at 75°C. External analytical precision for $\delta^{13}\text{C}$ measurements on samples of *O. universa* final chamber fragments is $\pm 0.06\text{‰}$ (2 SD). Sample weights (10–90 µg) were comparable

between the GSMS analyses run in the UCSC and UCD laboratories.

For comparative purposes, three samples of the UWC-3 standard were analyzed by GSMS at both UCSC and UCD. For the analyses at UCSC, each sample weighed 70–90 µg and was composed of 2–5 calcite grains. At UCD, each sample was composed of a single grain that weighed 33–40 µg. The GSMS $\delta^{13}\text{C}$ values of the UWC-3 standard measured at UCSC and UCD were subsequently compared to those previously measured by GSMS at the University of Wisconsin-Madison.³³

2.5 | Determination of $\Delta^{13}\text{C}_{\text{SIMS-GSMS}}$

The $\Delta^{13}\text{C}_{\text{SIMS-GSMS}}$ values for each experiment were determined via a paired *t*-test on SIMS and GSMS $\delta^{13}\text{C}$ values. To account for the variable precision (0.4–1.3‰, average = 0.8‰, 2 SD) of some SIMS measurements, the SIMS $\delta^{13}\text{C}$ values were first bootstrapped 1000 times in R³⁵ using the measured $\delta^{13}\text{C}$ value and the associated precision (2 SD). This methodology output 1000 paired datasets of bootstrapped SIMS $\delta^{13}\text{C}$ values and measured GSMS $\delta^{13}\text{C}$ values for each shell. A *t*-test was completed on each set of paired $\delta^{13}\text{C}$ values, yielding 1000 *t*-test estimates and 1000 *p*-values, which indicate the difference in $\delta^{13}\text{C}$ values and statistical significance of this difference, respectively. The $\Delta^{13}\text{C}_{\text{SIMS-GSMS}}$ value for each experiment is the average *t*-test estimate after bootstrapping. Similar $\Delta^{13}\text{C}_{\text{SIMS-GSMS}}$ values result from comparison of the average SIMS $\delta^{13}\text{C}$ value with the average GSMS $\delta^{13}\text{C}$ value for each experiment. The benefit of the bootstrapping approach, however, is that it provides a more rigorous assessment of the error and statistical significance of the $\Delta^{13}\text{C}_{\text{SIMS-GSMS}}$ values by accounting for the variable error on SIMS $\delta^{13}\text{C}$ measurements.

3 | RESULTS

3.1 | Comparison of paired SIMS–GSMS $\delta^{13}\text{C}$ analyses

The $\delta^{13}\text{C}$ measurement of foraminifer calcite by SIMS is standardized to the GSMS-derived $\delta^{13}\text{C}$ value of the UWC-3 calcite standard, assuming that the IMFs are equivalent. For this reason, we first analyzed the UWC-3 standard by GSMS in the same laboratories that measured the $\delta^{13}\text{C}$ compositions of *O. universa* chamber fragments. GSMS $\delta^{13}\text{C}$ values of UWC-3 analyzed by UCSC ($-0.9 \pm 0.1\text{‰}$, 2 SE) and UCD ($-1.0 \pm 0.2\text{‰}$) are within analytical precision of the published value ($-0.9 \pm 0.1\text{‰}$)³³ used for instrumental correction of the raw SIMS data (Table 1). We note that the samples of UWC-3 used for GSMS measurements at UCSC and UCD were of a comparable size to fragmented foraminifer chambers (30–40 µg) and reproduced the established UWC-3 $\delta^{13}\text{C}$ value to within 0.1‰.

The differing spatial resolutions (7 versus 10–50 µm), weights (10^{-5} versus ~ 30 µg), and volumes (30 versus $\sim 10^7$ µm³) of material

TABLE 1 GSMS $\delta^{13}\text{C}$ values for UWC-3 calcite. GSMS measurements performed at the University of Wisconsin-Madison established the $\delta^{13}\text{C}$ value ($-0.9 \pm 0.1\text{\textperthousand}$, 2 SD) for UWC-3 calcite.³³

Laboratory	Number of grains per analysis	Number of analyses	Sample weight (μg)	$\delta^{13}\text{C}$ (‰)		
				Average	2 SD	2 SE
University of Wisconsin-Madison	1–10	9	4000–8000	-0.9	0.1	<0.1
University of California Santa Cruz	2–5	3	73–91	-0.9	0.1	0.1
University of California Davis	1	3	31–40	-1.0	0.3	0.2

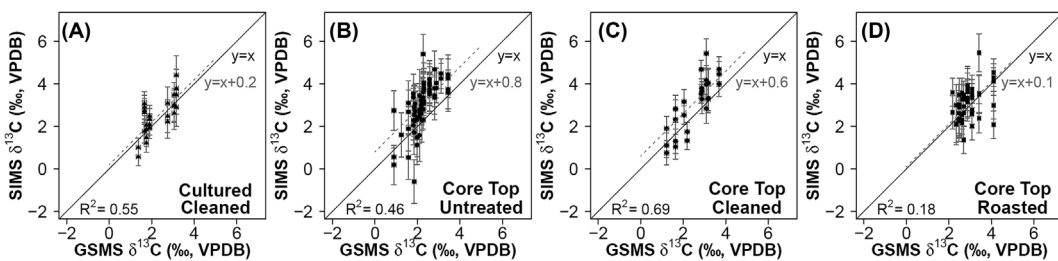


FIGURE 2 Comparison of paired SIMS and GSMS $\delta^{13}\text{C}$ values from the same final chamber of *Orbulina universa* shells. Theoretical 1-to-1 lines (solid bold lines) denote no difference between paired SIMS and GSMS $\delta^{13}\text{C}$ values for same final chamber. Linear regression with slope = 1 (dashed lines) fit to data. (A) Cleaned shells from culture experiment, (B) untreated core-top shells, (C) cleaned core-top shells, (D) vacuum-roasted core-top shells. All SIMS data shown are $\delta^{13}\text{C}$ values for individual pits. Error bars are analytical precision ($\pm 2\text{ SD}$) for GSMS (horizontal) and SIMS (vertical). VPDB, Vienna Pee Dee Belemnite.

analyzed by SIMS and GSMS techniques necessitated numerous *in situ* analyses for a robust comparison to the paired GSMS $\delta^{13}\text{C}$ measurement. On average, four *in situ* measurements were taken across the wall of the final chambers (Figure 1D). Although no $\delta^{13}\text{C}$ trends were apparent across the shell walls, the intrashell $\delta^{13}\text{C}$ variability varied markedly between the final chambers of different specimens ($\sim 0\text{--}3.5\text{\textperthousand}$) and SIMS measurements had larger errors ($\pm 0.8\text{\textperthousand}$ on average, 2 SD) in comparison to GSMS ($<0.1\text{\textperthousand}$, 2 SD). For these reasons, each SIMS $\delta^{13}\text{C}$ value was compared to the paired GSMS $\delta^{13}\text{C}$ value to ensure any interinstrument differences were not obfuscated by the averaging and propagating of errors for “per-shell” SIMS measurements.

The $\Delta^{13}\text{C}_{\text{SIMS-GSMS}}$ values for each experiment were determined by bootstrapping the SIMS $\delta^{13}\text{C}$ values and applying a paired *t*-test to the SIMS-GSMS datasets (see Section 2.5 for method details). Accordingly, paired SIMS and GSMS analyses performed on the cultured *O. universa* chambers ($n = 7$ shells) yield no discernible interinstrument $\delta^{13}\text{C}$ difference ($p > 0.05$; Figure 2A, Table 2). By contrast, the untreated ($n = 18$ shells) and cleaned ($n = 12$ shells) chamber fragments of fossil shells preserved in the PC9 core-top sample have $\Delta^{13}\text{C}_{\text{SIMS-GSMS}}$ values of $0.8\text{\textperthousand}$ and $0.6\text{\textperthousand}$, respectively (Table 2, Figures 2B and 2C). Interestingly, a third experimental design indicates that vacuum roasting of chamber fragments removes the SIMS-GSMS $\delta^{13}\text{C}$ offset registered by the core-top shells as the vacuum-roasted chambers have SIMS and GSMS $\delta^{13}\text{C}$ values that are statistically indistinguishable from one another ($\Delta^{13}\text{C}_{\text{SIMS-GSMS}} = 0.2 \pm 0.2\text{\textperthousand}$, $p > 0.05$; Figure 2D, Table 2). Another noteworthy finding is that SIMS and GSMS $\delta^{13}\text{C}$ values are positively

correlated, with a slope of unity, over the $\sim 2.5\text{\textperthousand}$ range of $\delta^{13}\text{C}$ values obtained from different *O. universa* final chambers in all experiments (Figure 2) and track one another as constrained by the 95% confidence interval of the slope ($m \approx 1$) (Table A2).

Due to the relatively small sample size (<20 shells), it is difficult to determine if hydrogen peroxide cleaning and sonication had an appreciable effect on the $\delta^{13}\text{C}$ values measured by either analytical technique, but results indicate that cleaning has no measurable effect on SIMS CH/C ratios relative to uncleared samples (Figure 3). To assess the effects of vacuum roasting, we compared the paired GSMS $\delta^{13}\text{C}$ values measured from vacuum-roasted and unroasted fragments of the same chamber (Figure 4). This direct comparison removes uncertainties related to intershell variability and indicates that vacuum roasting has no effect on GSMS $\delta^{13}\text{C}$ values (paired *t*-test $p = 0.4$; see Figure 4, Table A3). Thus, in comparison to the other experiments on core top shells, vacuum roasting must decrease SIMS $\delta^{13}\text{C}$ values to explain the improved agreement between SIMS and GSMS $\delta^{13}\text{C}$ values (Figure 2D, Table 2). The effect of vacuum roasting on SIMS measurements is further evidenced by the CH/C ratios of vacuum-roasted chambers, which are 20% lower than those of untreated, cleaned, and cultured chambers (Figure 3).

4 | DISCUSSION

The objective of this study was to quantify the $\delta^{13}\text{C}$ difference between SIMS and GSMS measurement techniques and determine the effect of sample treatment on said difference via paired analysis

TABLE 2 Summary of paired SIMS and GSMS $\delta^{13}\text{C}$ measurements of cleaned chambers from the PC9 core top, cleaned chambers from the PC9 core top, and vacuum-roasted chambers from the PC9 core top. Number of shells (n) analyzed by GSMS and number of pits (n) analyzed by SIMS noted for in each experimental group. The $\Delta^{13}\text{C}_{\text{SIMS-GSMS}}$ is the average (± 2 SD) SIMS–GSMS difference defined by the t -statistic output by the paired t -test performed on the bootstrapped datasets (see Section 2.5 for details). A p -value less than 0.05 indicates the SIMS–GSMS $\delta^{13}\text{C}$ difference is statistically significant at a 95% confidence interval (CI). Average CH/C ratios are background-corrected (± 2 SE).

Sample	Description	n	Average $\delta^{13}\text{C}$ (‰, VPDB)		$\Delta^{13}\text{C}_{\text{SIMS-CSMS}}$ (‰) ^a	SIMS versus GSMS $\delta^{13}\text{C}$ p [95% CI]	Average $^{13}\text{CH/}^{13}\text{C}$	Intrashell $\delta^{13}\text{C}$ range (‰) [\bar{x} = mean] ^b	
			SIMS	GSMS					
Culture	Hydrogen peroxide cleaned	27	7	2.5 ± 0.3	2.3 ± 0.3	0.2 ± 0.3	0.25 [0.24–0.27]	0.010 ± 0.002	0.4–1.5 [\bar{x} = 0.9]
PC9 (0–1 cm)	Untreated	85	18	2.9 ± 0.2	2.2 ± 0.1	0.8 ± 0.2	$2.0 \times 10^{-5^*}$ [1.4–2.6] $\times 10^{-5}$	0.010 ± 0.001	0.2–3.5 [\bar{x} = 1.4]
	Hydrogen peroxide cleaned, sonicated	32	12	3.0 ± 0.4	2.5 ± 0.3	0.6 ± 0.2	0.009* [0.0008–0.011]	0.010 ± 0.001	0–2.6 [\bar{x} = 0.8]
	Vacuum roasted	46	11	3.0 ± 0.2	2.9 ± 0.2	0.1 ± 0.2	0.41 [0.40–0.43]	0.008 ± 0.001	0.8–3.1 [\bar{x} = 1.5]

VPDB, Vienna Pee Dee Belemnite.

^aDefined as the mean t-statistic from the pa

^bIntrashell $\delta^{13}\text{C}$ range measured by SIMS.

ເຈລະຍະ/ ຈຳກັດ ແກ້ວມະນຸຍາ ແລະ ສະເພາະ ສະຫະລຸງ

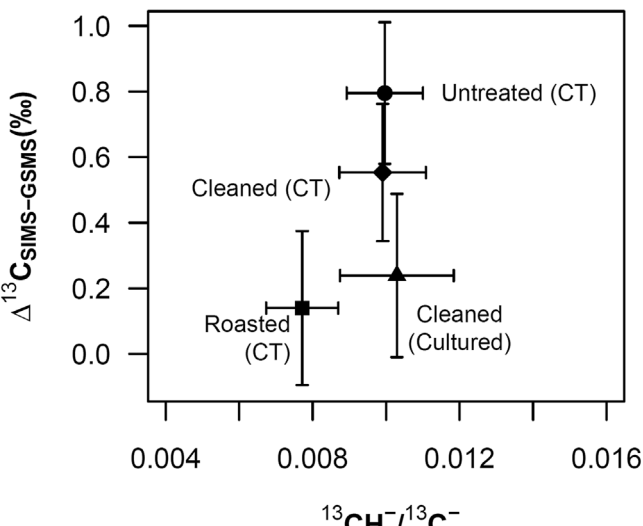


FIGURE 3 Average $\Delta^{13}\text{C}_{\text{SIMS-GSMS}}$ values plotted against background-corrected CH/C ratios measured for *Orbulina universa* chambers that were untreated (circle), cleaned with hydrogen peroxide and sonication (diamond), and vacuum roasted (square) from the Site PC9 core top (CT), as well as for cultured *O. universa* chambers cleaned with hydrogen peroxide (triangle). Error bars are two times the standard error of the CH/C ratio mean (horizontal) and two times the standard deviation of the $\Delta^{13}\text{C}_{\text{SIMS-GSMS}}$ mean (vertical).

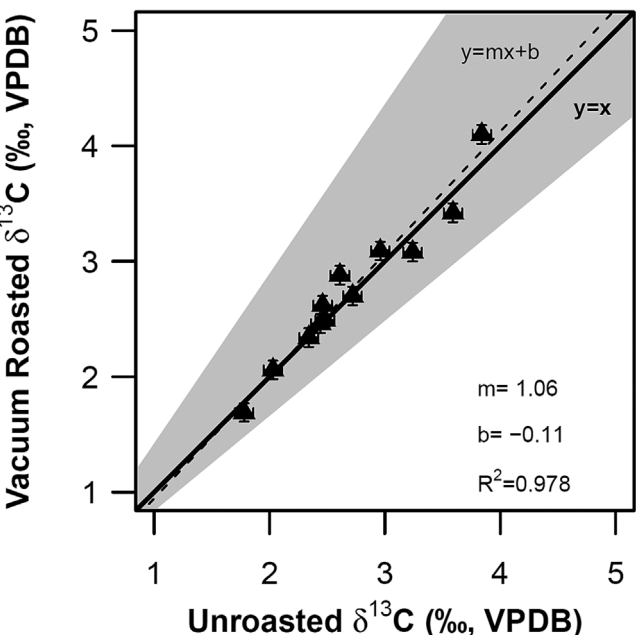


FIGURE 4 Comparison of GSMS $\delta^{13}\text{C}$ values measured from unroasted and vacuum-roasted fragments of the same *Orbulina universa* shell. Robust regression shown using iteratively reweighted least squares (dashed line) with corresponding slope (m) and y-intercept (b). Gray shading indicates 95% confidence interval on the slope (0.9 to 1.2) and y-intercept (−0.5 to 0.3). R^2 was calculated from unweighted least squares regression. Solid line indicates theoretical 1-to-1 line denoting no difference between GSMS $\delta^{13}\text{C}$ values of unroasted and vacuum-roasted fragments. Error bars express external instrumental precision ($\pm 2\text{ SD}$). VPDB, Vienna Pee Dee Belemnite.

of identical foraminifer material. SIMS $\delta^{13}\text{C}$ values closely track GSMS $\delta^{13}\text{C}$ values across the full population range of $\delta^{13}\text{C}$ values observed in the different experiments with a slope of unity (Figure 2), indicating that both analytical techniques record the same range of values for the selected *O. universa* shells. Moreover, SIMS $\delta^{13}\text{C}$ values are statistically indistinguishable from $\delta^{13}\text{C}$ values measured by GSMS on the calcite of the same *O. universa* spherical shells grown in laboratory culture (Figure 2A). These lines of evidence suggest that *in situ* SIMS measurements can be used to determine the $\delta^{13}\text{C}$ compositions of minute subdomains within individual fossil foraminifer shells or to generate $\delta^{13}\text{C}$ records based on diminutive foraminifer shells that are too small to be analyzed by GSMS methodologies. Yet, $\delta^{13}\text{C}$ values measured by SIMS on untreated or cleaned fossil shells are respectively $\sim 0.8\text{\textperthousand}$ and $\sim 0.6\text{\textperthousand}$ more positive than $\delta^{13}\text{C}$ values returned by GSMS of calcite from the same final chambers of fossil *O. universa* shells preserved in deep-sea sediments (Figures 2B and 2C). Below, we evaluate possible explanations for the SIMS–GSMS $\delta^{13}\text{C}$ differences recorded by the fossil shells analyzed in this study that can be eliminated by sample roasting *in vacuo*.

4.1 | SIMS–GSMS $\delta^{13}\text{C}$ difference

The interinstrument differences reported in this study may arise from both GSMS analyses entailing acid digestion of bulk carbonate and *in situ* SIMS analyses that subsample micrometer-scaled domains within an individual shell. Both techniques have the potential to capture differing $\delta^{13}\text{C}$ signals due to the disparate analytical setups and sample sizes. Further, we note that SIMS analyses entail the isolated measurement of micrometer-scale targets, which permits the operator to avoid irregular or altered domains. Conversely, numerous SIMS measurements may be required for robust comparison to the paired GSMS $\delta^{13}\text{C}$ value. Thus, SIMS $\delta^{13}\text{C}$ values may not fully capture the bulk $\delta^{13}\text{C}$ composition of larger samples measured by GSMS.

4.2 | $\delta^{13}\text{C}$ signals captured by GSMS

GSMS is the established, traditional technique used for $\delta^{13}\text{C}$ measurement of foraminifer calcite. The two GSMS laboratories that analyzed *O. universa* chambers reproduced the $\delta^{13}\text{C}$ value of the UWC-3 standard to within $0.1\text{\textperthousand}$ of the published value obtained at University of Wisconsin³³ even though the measurements were performed using different acid-digestion temperatures and instrumental setups (Kiel device at 75°C versus common acid bath at 90°C). Furthermore, foraminifer sample roasting *in vacuo* does not affect $\delta^{13}\text{C}$ values measured by the acid-digestion technique given that paired untreated and vacuum-roasted *O. universa* fragments have statistically indistinguishable GSMS $\delta^{13}\text{C}$ values (Figure 4, Table A3). Overall, the results of the UWC-3 analyses and vacuum roasting experiment suggest that a negligible proportion of the measured $0.8\text{\textperthousand}$ SIMS–GSMS $\delta^{13}\text{C}$ difference registered by untreated fossil shells from the core-top sample can be attributed to GSMS analyses.

4.3 | Potential sources of $\Delta^{13}\text{C}_{\text{SIMS-GSMS}}$: Matrix effects

Stable isotope analysis by SIMS is a comparative technique that requires a reference material that matches the matrix of the sample in mineralogy, chemical composition, and microcrystalline texture.^{34,36–39} The biogenic processes by which foraminifers precipitate their shells^{40,41} are fundamentally different from the recrystallization that occurs in a granulite facies marble that formed the UWC-3 standard. This is noteworthy because these abiotic/biotic processes give rise to carbonates with different microstructures, and the data corrections to SIMS analyses performed in this study were standardized with the assumption that the IMF of the UWC-3 analyses matches that of the samples. This procedure is not ideal, but it is currently the best method to standardize SIMS measurements as there currently are no biogenic carbonates that are homogeneous for $\delta^{13}\text{C}$ on the scale required for *in situ* measurements ($< 10\text{ }\mu\text{m}$).

The intrashell $\delta^{13}\text{C}$ variability for the core-top shells ranges from 0 to $3.9\text{\textperthousand}$ (Table 2), which is notably larger than the 1\textperthousand range expected, based on the $\delta^{13}\text{C}_{\text{DIC}}$ in the upper water column above Site PC9.⁴² In addition, the intrashell $\delta^{13}\text{C}$ variability of the cultured shells that were grown under constant $\delta^{13}\text{C}_{\text{DIC}}$ ranges from 0.4 to $1.5\text{\textperthousand}$ (Table 2). Some of this $\delta^{13}\text{C}$ variability in cultured shells can be attributed to SIMS analysis of day–night banding of calcite, which might differ by up to $\sim 2\text{\textperthousand}$ based on culturing experiments of another planktic foraminifer species, *Trilobatus sacculifer*.¹⁴ However, the three *O. universa* shells cultured under 24 h low light levels still had intrashell $\delta^{13}\text{C}$ variabilities of $0.6\text{\textperthousand}$, $0.8\text{\textperthousand}$, and $1.3\text{\textperthousand}$ (Table S1). The large intrashell $\delta^{13}\text{C}$ variability in both cultured and core-top shells indicates the presence of a matrix effect on SIMS measurements.

Foraminifer $\delta^{13}\text{C}$ values measured with SIMS may be affected by carbon-bearing contaminant phases such as organics that have isotope ratios, IMF, and/or ionization potentials that differ from those of calcite. Furthermore, minor element composition is known to affect the IMF of SIMS analyses.^{43–45} While the effects of most minor elements ($< 0.5\text{ wt\%}$) on IMF are within analytical precision, the cation composition of calcite needs to be examined in more detail. This is especially true for minor element concentrations in the UWC-3 standard,³³ which are higher than in modern planktic foraminifers⁴⁶ and may cause IMF differences between the standard and sample.

The microcrystalline structure of foraminifer calcite may also affect IMF, thereby causing differences between SIMS $\delta^{13}\text{C}$ analyses of biogenic carbonate samples and a standard that crystallized at high temperatures. BSE SEM images of the *O. universa* shells in cross-section (Figure 5) reveal notable differences in foraminifer wall textures depending on the shell treatment. Specifically, the untreated and cleaned core-top shells have a uniform texture except for several bright bands running perpendicular to the growth direction (Figures 5A and 5B). By contrast, the cultured shells and the vacuum-roasted core-top shells have mottled shell wall textures (Figures 5C–5F). The similar textures among the shells that have a negligible SIMS–GSMS $\delta^{13}\text{C}$ difference (i.e. the cultured shells and the vacuum-roasted core-top shells) suggest that the matrices of

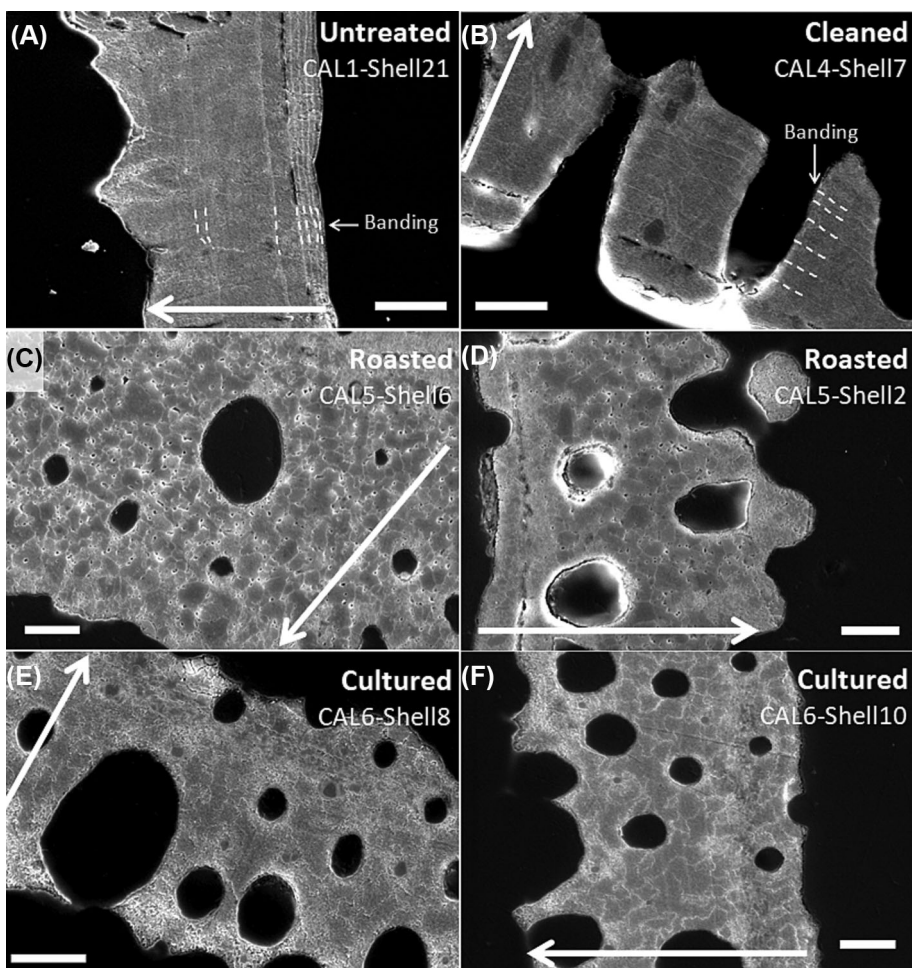


FIGURE 5 Highly magnified SE SEM images of *Orbulina universa* shells in cross-section. All images were obtained using the same SEM conditions. All scale bars are 10 μm . Arrows note direction of shell growth. (A) Untreated core-top shells and (B) cleaned core-top shells with bright banding perpendicular to the growth direction and otherwise uniform internal shell texture. (C, D) Vacuum-roasted core-top shells with mottled internal shell textures. (E, F) Cultured cleaned shells with mottled internal shell textures.

these shells have been chemically or physically altered making them microstructurally more comparable to the UWC-3 standard. Although the vacuum-roasted and cultured shells differ from the UWC-3 marble in organic content and minor element composition, the differences observed in the SEM images imply that microstructure likely plays a considerable role in SIMS $\delta^{13}\text{C}$ measurement of planktic foraminifers.

4.4 | Potential sources of $\Delta^{13}\text{C}_{\text{SIMS-GSMS}}$: SIMS measurement of matrix-bound organics or water

Organic compounds and water are not thought to contribute to the CO_2 analyzed by GSMS during phosphoric acid digestion, whereas SIMS $\delta^{13}\text{C}$ analysis involves the measurement of all organic and inorganic phases in the excavated SIMS pit. Thus, SIMS measurement of biogenic carbonates may be affected if organics or water are bound within the calcite matrix^{29,47} or if the organics occur as nanophases along grain boundaries.⁴⁸ The vacuum-roasting experiment was performed to remove volatile organic compounds and intracrystalline water, while leaving refractory compounds within the matrix. The *O. universa* fragments looked gray in color after vacuum roasting, evidence of organic carbon maturation. This observation implies

reaction, but ineffective removal of refractory organic contaminants. The CH/C ratios of vacuum-roasted chambers are $\sim 20\%$ lower than those of cultured, untreated, and cleaned chambers (Figure 3) at a statistically significant level ($p \ll 0.05$), indicating that a hydrogen-bearing phase such as organics and/or water was removed by vacuum roasting. Results from the SIMS-GSMS roasting experiment indicate that SIMS $\delta^{13}\text{C}$ values are more affected by vacuum roasting (Figures 2D and 4), but it is difficult to determine if this is due to reaction/removal of phases such as organics or water or if it is due to a change in IMF. The fact that unroasted (hydrated), organic-rich cultured shells have no measurable SIMS-GSMS $\delta^{13}\text{C}$ difference provides demonstrable evidence that SIMS-only measurement of organics or water cannot explain the positive $\Delta^{13}\text{C}_{\text{SIMS-GSMS}}$ values measured for unroasted core-top shells.

4.5 | Potential sources of $\Delta^{13}\text{C}_{\text{SIMS-GSMS}}$: Measurement of secondary calcite phases

Secondary calcite phases that could bias GSMS analyses of *O. universa* chambers from deep-sea sediment core PC9 are low- $\delta^{13}\text{C}$ gametogenic (GAM) and diagenetic calcite, which would be included in acid dissolution/GSMS analyses but avoided by carefully targeted

SIMS pits. Approximately 4 µg of GAM calcite is added to the outer surface of *O. universa* shells during the final 24 h of calcification near the deep chlorophyll maximum as the species transitions from its normal life through meiosis and gamete production.^{15,27} In addition, diagenesis can add submicrometer- to micrometer-scale carbonate phases onto foraminifer shells.^{8,9,19,49–52} The proximity of the thin GAM crust (~2 µm) and minute (<3 µm) early diagenetic crystallites to the mounting medium (epoxy) precludes measurement of their $\delta^{13}\text{C}$ by SIMS. The secondary calcite phases cannot be removed or separated prior to GSMS analysis and would contribute to the SIMS–GSMS $\delta^{13}\text{C}$ difference.

Although there is no SIMS–GSMS $\delta^{13}\text{C}$ difference measured for cultured shells that have the same GAM and pre-GAM calcite $\delta^{13}\text{C}$ values,²⁷ the addition of GAM crust is not a feasible explanation for the measured $\Delta^{13}\text{C}_{\text{SIMS-GSMS}}$ values (Table 2) because the GAM crust appears to compose a minute (<10%) portion of the shell wall (Dataset S2) and the required $\delta^{13}\text{C}$ value of the GAM calcite on untreated and cleaned shells (Table 2) is not realistic given there is less than a 1‰ range in the $\delta^{13}\text{C}$ of the DIC in the upper water column above Site PC9.⁴²

A salient result of this study is the similar SIMS and GSMS $\delta^{13}\text{C}$ values measured for the cultured chambers that have never been exposed to seafloor conditions. The shells recovered from the Site PC9 core-top presumably have similar burial histories and are therefore composed of comparable amounts of diagenetic calcite. Although the untreated and cleaned core-top shells have measurable $\Delta^{13}\text{C}_{\text{SIMS-GSMS}}$ values, there is no SIMS–GSMS $\delta^{13}\text{C}$ difference for the vacuum-roasted core-top shells. Therefore, the analysis of diagenetic calcite by only GSMS cannot explain patterns observed in the entire $\Delta^{13}\text{C}_{\text{SIMS-GSMS}}$ dataset.

5 | CONCLUSIONS

Prior to this study, the $\delta^{13}\text{C}$ values of planktic foraminifers have been measured by SIMS to understand the magnitude of carbon release in past climate events, diagenetic effects on marine climate records,^{19,23} and carbon uptake during biocalcification.²¹ However, the signals measured by SIMS can be different from those captured by conventional GSMS analysis. Paired $\delta^{13}\text{C}$ measurements were performed on the final chamber of the same *O. universa* shell using *in situ* SIMS and acid-digestion GSMS analyses, permitting the direct comparison of the two analytical techniques. Analyses of individual foraminifer chambers were carried out on specimens grown in laboratory culture and fossil (Holocene) shells collected from the upper 3 cm of a deep-sea sediment core (PC9). Comparison of the resulting data shows no difference between SIMS and GSMS $\delta^{13}\text{C}$ values of cultured *O. universa* shells cleaned with hydrogen peroxide. Yet, an average $\Delta^{13}\text{C}_{\text{SIMS-GSMS}}$ value of 0.8‰ and 0.6‰ is evident among the untreated and cleaned (hydrogen peroxide, sonicated) shells from the PC9 core-top, respectively. This interinstrument difference is removed by vacuum roasting of additional shells also selected from the PC9 core-top sample. Strong positive covariance

between the SIMS and GSMS values in all experiments of this study indicates that intershell $\delta^{13}\text{C}$ differences and secular trends expressed in foraminifer $\delta^{13}\text{C}$ records generated via conventional GSMS analyses are reproduced by SIMS analyses of age-equivalent foraminifers.

The interinstrument $\delta^{13}\text{C}$ differences measured in this study likely stem, in large part, from an imperfect match of the SIMS calcite standard to samples but may be a combination of this and other factors such as SIMS measurement of chemically bound water and GSMS measurement of a thin GAM or diagenetic crust. No SIMS standard presently exists that perfectly matches the samples of this study in terms of minor element concentration, amount and phase of the organic/hydrous component, and crystalline microstructure. Determining the roles of these various mechanisms in causing the interinstrument differences herein reported is beyond the scope of the present study. Furthermore, we caution that the $\Delta^{13}\text{C}_{\text{SIMS-GSMS}}$ values reported in this study may not be the same for $\delta^{13}\text{C}$ analyses performed in different SIMS sessions or on foraminifer taxa with substantially different compositions, shell microstructures, porosities, and/or burial histories. This is especially true for foraminifer shells recovered from older, more deeply buried sediments that have experienced a greater degree of geochemical alteration and recrystallization as diagenetic processes tend to degrade organic compounds⁵³ and increase the $\delta^{13}\text{C}$ value of the whole shell.^{9,49,50} Results of this study further highlight the unique signals captured by SIMS and GSMS, which should be considered for the experimental design of future studies.

AUTHOR CONTRIBUTIONS

Jody B. Wycech: Conceptualization; investigation; writing—original draft; methodology; validation; visualization; software; formal analysis; writing—review and editing; data curation. **Daniel Clay Kelly:** Investigation; writing—original draft; writing—review and editing; methodology; validation; project administration; supervision; resources; funding acquisition. **Reinhard Kozdon:** Writing—review and editing; investigation; funding acquisition; methodology; validation; data curation; formal analysis; project administration; supervision. **Akizumi Ishida:** Formal analysis. **Kouki Kitajima:** Formal analysis; writing—review and editing; data curation. **Howard J. Spero:** Writing—review and editing; investigation; methodology; validation; formal analysis; supervision; resources. **John W. Valley:** Writing—review and editing; investigation; funding acquisition; formal analysis; project administration; supervision; resources; methodology; validation.

ACKNOWLEDGMENTS

Any use of trade, firm, or product names is for descriptive purposes only and does not imply endorsement by the US Government. Funding was provided by NSF (OCE-1405224, D.C.K. and R.K.; OCE-0550703, H.S.). WiscSIMS is supported by NSF (EAR-1658823 and -2004618) and UW-Madison. J.V. was supported by DOE, Office of Basic Energy Sciences, Geosciences Division (DE-FG02-93ER14389). Shipboard coring operations were supported by the US Geological Survey (William Dillon) and Woods Hole Oceanographic Institute

(D.C.K., Richard Norris). The crew of the RV *Cape Hatteras*, Charles Paull, and William Ussler conducted coring operations. We thank Ellen Roosen (WHOI Core Repository) for core sampling assistance. Cultured shells were grown by C. Hamilton (UCD). Conventional stable isotope measurements were assisted by Dyke Andreasen (UCSC) and Edward Chu (UCD). Brian Hess prepared epoxy mounts. Noriko Kita assisted SIMS measurements. We thank Adam Denny, Benjamin Linzmeier, Maciej Sliwiński, and Nick Levitt for fruitful discussions.

PEER REVIEW

The peer review history for this article is available at <https://www.webofscience.com/api/gateway/wos/peer-review/10.1002/rcm.9658>.

DATA AVAILABILITY STATEMENT

The data that support the findings of this study are openly available in ScienceBase at <https://doi.org/10.5066/P9524ENX>.⁵⁴

ORCID

Jody B. Wycech  <https://orcid.org/0000-0002-7073-3037>
 Daniel Clay Kelly  <https://orcid.org/0000-0002-3241-1635>
 Reinhard Kozdon  <https://orcid.org/0000-0001-6347-456X>
 Akizumi Ishida  <https://orcid.org/0000-0002-1580-8534>
 Kouki Kitajima  <https://orcid.org/0000-0001-7634-4924>
 Howard J. Spero  <https://orcid.org/0000-0001-5465-8607>
 John W. Valley  <https://orcid.org/0000-0003-3530-2722>

REFERENCES

1. Ninnemann US, Charles CD. Changes in the mode of Southern Ocean circulation over the last glacial cycle revealed by foraminiferal stable isotopic variability. *Earth Planet Sci Lett.* 2002;201(2):383-396. doi:[10.1016/S0012-821X\(02\)00708-2](https://doi.org/10.1016/S0012-821X(02)00708-2)
2. Ravelo AC, Andreasen DH. Enhanced circulation during a warm period. *Geophys Res Lett.* 2000;27(7):1001-1004. doi:[10.1029/1999GL007000](https://doi.org/10.1029/1999GL007000)
3. Spero H, Mielke KM, Kalve EM, Lea DW, Pak DK. Multispecies approach to reconstructing eastern equatorial Pacific thermocline hydrography during the past 360 kyr. *Paleoceanography.* 2003;18(1):1-16. doi:[10.1029/2002PA000814](https://doi.org/10.1029/2002PA000814)
4. Doss W, Marchitto TM. Glacial deep ocean sequestration of CO₂ driven by the eastern equatorial Pacific biologic pump. *Earth Planet Sci Lett.* 2013;377-378(C):43-54. doi:[10.1016/j.epsl.2013.07.019](https://doi.org/10.1016/j.epsl.2013.07.019)
5. Sarnthein M, Winn K, Duplessy JC, Fontugne MR. Global variations of surface ocean productivity in low and mid latitudes: influence on CO₂ reservoirs of the deep ocean and atmosphere during the last 21,000 years. *Paleoceanography.* 1988;3(3):361-399. doi:[10.1029/PA003i003p00361](https://doi.org/10.1029/PA003i003p00361)
6. Kennett JP, Stott LD. Abrupt deep-sea warming, palaeoceanographic changes and benthic extinctions at the end of the Palaeocene. *Nature.* 1991;353(6341):225-229. doi:[10.1038/353225a0](https://doi.org/10.1038/353225a0)
7. Peterson CD, Lisiecki LE, Stern JV. Deglacial whole-ocean $\delta^{13}\text{C}$ change estimated from 480 benthic foraminiferal records. *Paleoceanography.* 2014;29:549-563. doi:[10.1002/1944-9186](https://doi.org/10.1002/1944-9186)
8. Killingley JS. Effects of diagenetic recrystallization on $^{18}\text{O}/^{16}\text{O}$ values of deep-sea sediments. *Nature.* 1983;301(5901):594-597. doi:[10.1038/301594a0](https://doi.org/10.1038/301594a0)
9. Pearson PN, Ditchfield PW, Singano J, et al. Warm tropical sea surface temperatures in the Late Cretaceous and Eocene epochs. *Nature.* 2001;413(6855):481-487. doi:[10.1038/35097000](https://doi.org/10.1038/35097000)
10. Schrag DP, DePaolo DJ, Richter FM. Reconstructing past sea surface temperatures: Correcting for diagenesis of bulk marine carbonate. *Geochim Cosmochim Acta.* 1995;59(11):2265-2278. doi:[10.1016/0016-7037\(95\)00105-9](https://doi.org/10.1016/0016-7037(95)00105-9)
11. Bemis BE, Spero HJ, Lea DW, Bijma J. Temperature influence on the carbon isotopic composition of *Globigerina bulloides* and *Orbulina universa* (planktonic foraminifera). *Mar Micropaleontol.* 2000;38(3-4):213-228. doi:[10.1016/S0377-8398\(00\)00006-2](https://doi.org/10.1016/S0377-8398(00)00006-2)
12. Ortiz JD, Mix AC, Rugh W, Watkins JM, Collier RW. Deep-dwelling planktonic foraminifera of the northeastern Pacific Ocean reveal environmental control of oxygen and carbon isotopic disequilibria. *Geochim Cosmochim Acta.* 1996;60(22):4509-4523. doi:[10.1016/S0016-7037\(96\)00256-6](https://doi.org/10.1016/S0016-7037(96)00256-6)
13. Spero H, Lerche I, Williams DF. Opening the carbon isotope "vital effect" black box, 2, quantitative model for interpreting foraminiferal carbon isotope data. *Paleoceanography.* 1991;6(6):639-655. doi:[10.1029/91PA02022](https://doi.org/10.1029/91PA02022)
14. Spero H, Lea DW. Intraspecific stable isotope variability in the planktic foraminifera *Globigerinoides sacculifer*: Results from laboratory experiments. *Mar Micropaleontol.* 1993;22(3):221-234. doi:[10.1016/0377-8398\(93\)90045-Y](https://doi.org/10.1016/0377-8398(93)90045-Y)
15. Bé AW. Gametogenic calcification in a spinose planktonic foraminifer, *Globigerinoides sacculifer* (Brady). *Mar Micropaleontol.* 1980;5:283-310. doi:[10.1016/0377-8398\(80\)90014-6](https://doi.org/10.1016/0377-8398(80)90014-6)
16. Duplessy JC, Blanc PL, Bé AW. Oxygen-18 enrichment of planktonic foraminifera due to gametogenic calcification below the euphotic zone. *Science.* 1981;213(4513):1247-1250. doi:[10.1126/science.213.4513.1247](https://doi.org/10.1126/science.213.4513.1247)
17. Lohmann GP. A model for variation in the chemistry of planktonic foraminifera due to secondary calcification and selective dissolution. *Paleoceanography.* 1995;10(3):445-457. doi:[10.1029/95PA00059](https://doi.org/10.1029/95PA00059)
18. Rosenthal Y, Lohmann GP, Lohmann KC, Sherrell RM. Incorporation and preservation of Mg in *Globigerinoides sacculifer*: Implications for reconstructing the temperature and $^{18}\text{O}/^{16}\text{O}$ of seawater. *Paleoceanography.* 2000;15(1):135-145. doi:[10.1029/1999PA000415](https://doi.org/10.1029/1999PA000415)
19. Kozdon R, Kelly DC, Valley JW. Diagenetic attenuation of carbon isotope excursion recorded by planktic foraminifers during the Paleocene-Eocene thermal maximum. *Paleoceanogr Paleoclimatol.* 2018;369(3):1-14. doi:[10.1016/j.gr.2017.02.016](https://doi.org/10.1016/j.gr.2017.02.016)
20. Limburg KE, Hayden TA, Pine WE, Yard MD, Kozdon R, Valley JW. Of travertine and time: Otolith chemistry and microstructure detect provenance and demography of endangered humpback chub in Grand Canyon, USA. *PLoS ONE.* 2013;8(12):e84235. doi:[10.1371/journal.pone.0084235](https://doi.org/10.1371/journal.pone.0084235)
21. Vetter L, Kozdon R, Valley JW, Mora CI, Spero HJ. SIMS measurements of intrashell $\delta^{13}\text{C}$ in the cultured planktic foraminifer *Orbulina universa*. *Geochim Cosmochim Acta.* 2014;139(C):527-539. doi:[10.1016/j.gca.2014.04.049](https://doi.org/10.1016/j.gca.2014.04.049)
22. Weidel BC, Ushikubo T, Carpenter SR, et al. Diary of a bluegill (*Lepomis macrochirus*): Daily $\delta^{13}\text{C}$ and $\delta^{18}\text{O}$ records in otoliths by ion microprobe. *Can J Fish Aquat Sci.* 2007;64(12):1641-1645. doi:[10.1139/f07-157](https://doi.org/10.1139/f07-157)
23. Hupp BN, Kelly DC, Kozdon R, Orland IJ, Valley JW. Secondary controls on the stratigraphic signature of the carbon isotope excursion marking the Paleocene-Eocene thermal maximum at Ocean Drilling Program Site 1135. *Chem Geol.* 2023;632:121534. doi:[10.1016/j.chemgeo.2023.121534](https://doi.org/10.1016/j.chemgeo.2023.121534)
24. Hemleben C, Spindler M, Anderson OR. *Modern Planktonic Foraminifera*. Springer-Verlag; 1989. doi:[10.1007/978-1-4612-3544-6](https://doi.org/10.1007/978-1-4612-3544-6)
25. Spero H, Parker SL. Photosynthesis in the symbiotic planktonic foraminifer *Orbulina universa*, and its potential contribution to oceanic

primary productivity. *J Foraminiferal Res.* 1985;15(4):273-281. doi:[10.2113/gsjfr.15.4.273](https://doi.org/10.2113/gsjfr.15.4.273)

26. Birch H, Coxall HK, Pearson PN, Kroon D, O'Regan M. Planktonic foraminifera stable isotopes and water column structure: Disentangling ecological signals. *Mar Micropaleontol.* 2013;101(C): 127-145. doi:[10.1016/j.marmicro.2013.02.002](https://doi.org/10.1016/j.marmicro.2013.02.002)

27. Hamilton CP, Spero HJ, Bijma J, Lea DW. Geochemical investigation of gametogenic calcite addition in the planktonic foraminifera *Orbulina universa*. *Mar Micropaleontol.* 2008;68(3-4):256-267. doi:[10.1016/j.marmicro.2008.04.003](https://doi.org/10.1016/j.marmicro.2008.04.003)

28. Bé AW, Harrison S, Lott L. *Orbulina universa* d'Orbigny in the Indian Ocean. *Micropaleontology.* 1973;19(2):150-192. doi:[10.2307/1485162](https://doi.org/10.2307/1485162)

29. Spero H. Ultrastructural examination of chamber morphogenesis and biomineralization in the planktonic foraminifer *Orbulina universa*. *Mar Biol.* 1988;99(1):9-20. doi:[10.1007/BF00644972](https://doi.org/10.1007/BF00644972)

30. Fehrenbacher JS, Spero HJ, Russell AD, Vetter L, Eggins S. Optimizing LA-ICP-MS analytical procedures for elemental depth profiling of foraminifera shells. *Chem Geol.* 2015;407-408(C):2-9. doi:[10.1016/j.chemgeo.2015.04.007](https://doi.org/10.1016/j.chemgeo.2015.04.007)

31. Bemis BE, Spero HJ, Bijma J, Lea DW. Reevaluation of the oxygen isotopic composition of planktonic foraminifera: Experimental results and revised paleotemperature equations. *Paleoceanography.* 1998; 13(2):150-160. doi:[10.1029/98PA00070](https://doi.org/10.1029/98PA00070)

32. Wycech J, Kelly DC, Marcott S. Effects of seafloor diagenesis on planktic foraminiferal radiocarbon ages. *Geology.* 2016;44(7):551-554. doi:[10.1130/G37864.1](https://doi.org/10.1130/G37864.1)

33. Kozdon R, Ushikubo T, Kita NT, Spicuzza MJ, Valley JW. Intratest oxygen isotope variability in the planktonic foraminifer *N. pachyderma*: Real vs. apparent vital effects by ion microprobe. *Chem Geol.* 2009;258(3-4):327-337. doi:[10.1016/j.chemgeo.2008.10.032](https://doi.org/10.1016/j.chemgeo.2008.10.032)

34. Kita NT, Ushikubo T, Fu B, Valley JW. High precision SIMS oxygen isotope analysis and the effect of sample topography. *Chem Geol.* 2009;264(1-4):43-57. doi:[10.1016/j.chemgeo.2009.02.012](https://doi.org/10.1016/j.chemgeo.2009.02.012)

35. R Core Team. R: a language and environment for statistical computing. 2021. Accessed September 13, 2022. <https://www.R-project.org>

36. Eiler JM, Graham CM, Valley JW. SIMS analysis of oxygen isotopes: Matrix effects in complex minerals and glasses. *Chem Geol.* 1997; 138(3-4):221-244. doi:[10.1016/S0009-2541\(97\)00015-6](https://doi.org/10.1016/S0009-2541(97)00015-6)

37. Fitzsimons ICW, Harte B, Clark RM. SIMS stable isotope measurement: Counting statistics and analytical precision. *Mineral Mag.* 2000;64(1):59-83. doi:[10.1180/002646100549139](https://doi.org/10.1180/002646100549139)

38. Hervig RL, Williams P, Thomas RM, Schauer SN, Steele IM. Microanalysis of oxygen isotopes in insulators by secondary ion mass spectrometry. *Int J Mass Spectrom.* 1992;120(1-2):45-63. doi:[10.1016/0168-1176\(92\)80051-2](https://doi.org/10.1016/0168-1176(92)80051-2)

39. Huberty JM, Kita NT, Kozdon R, et al. Crystal orientation effects in $\delta^{18}\text{O}$ for magnetite and hematite by SIMS. *Chem Geol.* 2010; 276(3-4):269-283. doi:[10.1016/j.chemgeo.2010.06.012](https://doi.org/10.1016/j.chemgeo.2010.06.012)

40. de Nooijer LJ, Spero HJ, Erez J, Bijma J, Reichart GJ. Biomineralization in perforate foraminifera. *Earth Sci Rev.* 2014; 135(C):48-58. doi:[10.1016/j.earscirev.2014.03.013](https://doi.org/10.1016/j.earscirev.2014.03.013)

41. Jacob DE, Wirth R, Agbaje OBA, Branson O, Eggins SM. Planktic foraminifera form their shells via metastable carbonate phases. *Nat Commun.* 2017;8(1):1265. doi:[10.1038/s41467-017-00955-0](https://doi.org/10.1038/s41467-017-00955-0)

42. Kroopnick PM. The distribution of ^{13}C of ΣCO_2 in the world oceans. *Deep-Sea Res II.* 1985;32(1):57-84. doi:[10.1016/0198-0149\(85\)90017-2](https://doi.org/10.1016/0198-0149(85)90017-2)

43. Eiler JM, Valley JW, Graham CM, Fournelle J. Two populations of carbonate in ALH84001: Geochemical evidence for discrimination and genesis. *Geochim Cosmochim Acta.* 2002;66(7):1285-1303. doi:[10.1016/S0016-7037\(01\)00847-X](https://doi.org/10.1016/S0016-7037(01)00847-X)

44. Valley J, Kita N. *In situ* oxygen isotope geochemistry by ion microprobe. Paper presented at: Mineralogical Association of Canada Short Course 41; May 2009; Toronto, Canada.

45. Śliwiński M, Kitajima K, Spicuzza MJ, et al. SIMS bias on isotope ratios in Ca-Mg-Fe carbonates (part III): $\delta^{18}\text{O}$ and $\delta^{13}\text{C}$ matrix effects along the magnesite-siderite solid-solution series. *Geostand Geoanal Res.* 2018;42(1):49-76. doi:[10.1111/ggr.12194](https://doi.org/10.1111/ggr.12194)

46. Wycech JB, Kelly DC, Kozdon R, Orland IJ, Spero HJ, Valley JW. Comparison of $\delta^{18}\text{O}$ analyses on individual planktic foraminifer (*Orbulina universa*) shells by SIMS and gas-source mass spectrometry. *Chem Geol.* 2018;483:119-130. doi:[10.1016/j.chemgeo.2018.02.028](https://doi.org/10.1016/j.chemgeo.2018.02.028)

47. Helser TE, Kastelle CR, McKay JL, Orland IJ, Kozdon R, Valley JW. Evaluation of micromilling/conventional isotope ratio mass spectrometry and secondary ion mass spectrometry of $\delta^{18}\text{O}$ values in fish otoliths for sclerochronology. *Rapid Commun Mass Spectrom.* 2018;32(20):1781-1790. doi:[10.1002/rcm.8231](https://doi.org/10.1002/rcm.8231)

48. Cuif JP, Dauphin Y, Nehrke G, Nouet J, Perez-Huerta A. Layered growth and crystallization in calcareous biominerals: Impact of structural and chemical evidence on two major concepts in invertebrate biomineralization studies. *Minerals.* 2012;2(4):11-39. doi:[10.1021/ac2017663](https://doi.org/10.1021/ac2017663)

49. Edgar KM, Agagnostou E, Pearson PN, Foster GL. Assessing the impact of diagenesis on $\delta^{11}\text{B}$, $\delta^{13}\text{C}$, $\delta^{18}\text{O}$, Sr/Ca and B/Ca values in fossil planktic foraminiferal calcite. *Geochim Cosmochim Acta.* 2015; 166(C):189-209. doi:[10.1016/j.gca.2015.06.018](https://doi.org/10.1016/j.gca.2015.06.018)

50. Kozdon R, Kelly DC, Kitajima K, Strickland A, Fournelle JH, Valley JW. *In situ* $\delta^{18}\text{O}$ and Mg/Ca analyses of diagenetic and planktic foraminiferal calcite preserved in a deep-sea record of the Paleocene-Eocene thermal maximum. *Paleoceanography.* 2013;28(3):517-528. doi:[10.1002/palo.20048](https://doi.org/10.1002/palo.20048)

51. Pearson PN, van Dongen BE, Nicholas CJ, et al. Stable warm tropical climate through the Eocene epoch. *Geology.* 2007;35(3):211-214. doi:[10.1130/G23175A.1](https://doi.org/10.1130/G23175A.1)

52. Sexton PF, Wilson PA, Pearson PN. Microstructural and geochemical perspectives on planktic foraminiferal preservation: "Glassy" versus "Frosty". *Geochim Geophys.* 2006;7(12):1-29. doi:[10.1029/2006GC001291](https://doi.org/10.1029/2006GC001291)

53. Gaffey S. Skeletal versus nonbiogenic carbonates UV-visible-near IR (0.3-2.7 μm) reflectance properties. In: Coyne LM, McKeever SW, Blake ES, eds. *Spectroscopic Characterization of Minerals and Their Surfaces.* Vol.415. American Chemical Society; 1990:94-116. doi:[10.1021/bk-1990-0415.ch005](https://doi.org/10.1021/bk-1990-0415.ch005)

54. Wycech JB, Kelly DC, Ishida A, et al. The $\delta^{13}\text{C}$ dataset of individual foraminifer (*Orbulina universa*) shells measured by secondary ion mass spectrometry and gas-source mass spectrometry. US Geological Survey data release; 2023. doi:[10.5066/P9524ENX](https://doi.org/10.5066/P9524ENX)

SUPPORTING INFORMATION

Additional supporting information can be found online in the Supporting Information section at the end of this article.

How to cite this article: Wycech JB, Kelly DC, Kozdon R, et al. Comparison of $\delta^{13}\text{C}$ analyses of individual foraminifer (*Orbulina universa*) shells by secondary ion mass spectrometry and gas source mass spectrometry. *Rapid Commun Mass Spectrom.* 2024;38(2):e9658. doi:[10.1002/rcm.9658](https://doi.org/10.1002/rcm.9658)

APPENDIX A

SIMS $\delta^{13}\text{C}$ data processing

The quality of each SIMS $\delta^{13}\text{C}$ analysis was evaluated on the basis of pit appearance by SEM (Figure A2) and secondary ion ($^{12}\text{C}^-$) count rate. The pit appearance and paired $\delta^{13}\text{C}$ value were each assigned a score from 1 to 3 (good = 1, questionable = 2, irregular = 3) using a method that was blind to the other metric, that is, pit appearance was scored without knowing the corresponding $\delta^{13}\text{C}$ value and vice versa. Pits were given a score of 2 if they had morphology that notably differed from the standard (Figure A2C) and a score of 3 if they had crosscut cracks or highly irregular internal structure (Figure A2D). The latter suggests that the pit intersected porous domains (epoxy), inclusions, or voids.

Epoxy is enriched in $^{12}\text{C}^-$, so sputtering through porous domains by SIMS can elevate the $^{12}\text{C}^-$ count rate of an analysis. The data quality of each foraminifer analysis was assessed by comparing the $^{12}\text{C}^-$ count rates between the analysis and the average $^{12}\text{C}^-$ count rate of the bracketing standards (i.e. count rate_{sample}/count rate_{bracketing-standards}). A datum was deemed acceptable (data quality score = 1) if it was below a count rate cutoff value. This cutoff value was defined as the rate 5% higher than the upper 2 standard deviation of the UWC-3 count rates measured for that session. However, if the $^{12}\text{C}^-$ count rate exceeded the cutoff value, the datum was excluded (data quality score = 3). It should also be noted that outliers only occurred at high $^{12}\text{C}^-$ count rates – SIMS analyses of foraminifers did not have $^{12}\text{C}^-$ count rates below the range of $^{12}\text{C}^-$ count rates measured for the standard in each run.

TABLE A1 Culturing conditions of *Orbulina universa* specimens used in this study. Measured SIMS $\delta^{13}\text{C}$ values are reported in Table S1. Measured GSMS $\delta^{13}\text{C}$ values are reported in Table S2.

Light cycle	ID (Spero Lab)	GSMS ID (this study)
12 h:12 h low light:dark	CH303, CH302	CS1, CS2
24 h low light	CH60, CH61, CH62	CS4, CS5, CS6
12 h:12 h high light:dark	CH114, CH122, CH124	CS7, CS8, CS9

TABLE A2 Slope, y-intercept, and 95% confidence interval (CI) provided by iteratively reweighted least squares regression (i.e. robust regression) analysis of GSMS $\delta^{13}\text{C}$ values versus SIMS $\delta^{13}\text{C}$ values for all experiments. The 95% CIs on all slopes include 1 so the $\Delta^{13}\text{C}_{\text{SIMS-GSMS}}$ values shown in Table 2 were defined as the SIMS versus GSMS $\delta^{13}\text{C}$ difference (assuming a slope of 1).

Sample	Description	Slope	95% CI	y-Intercept	95% CI
Culture	Hydrogen peroxide cleaned	0.9	0.6 to 1.3	0.3	-0.6 to 1.2
PC9 (0–3 cm)	Untreated	1.2	0.9 to 1.5	0.3	-0.4 to 0.9
	Hydrogen peroxide cleaned, sonicated	1.3	0.9 to 1.6	-0.2	-1.0 to 0.7
	Vacuum roasted	0.6	0.3 to 1.0	1.2	0.1 to 2.3

TABLE A3 GSMS $\delta^{13}\text{C}$ data for vacuum-roasted and unroasted fragments of the same *Orbulina universa* shell (>355 μm size fraction). Analytical precision is 0.08‰ (2 SD).

GSMS ID	Vacuum roasted $\delta^{13}\text{C}$ (‰, VPDB)	Unroasted $\delta^{13}\text{C}$ (‰, VPDB)
S1	2.70	2.72
S2	3.09	2.96
S4	4.10	3.84
S5	3.08	3.24
S6	1.69	1.78
S7	2.46	2.44
S8	2.34	2.34
S9	2.88	2.61
S10	3.42	3.59
S11	2.06	2.03
S12	2.62	2.46
S13	2.49	2.48

VPDB, Vienna Pee Dee Belemnite.

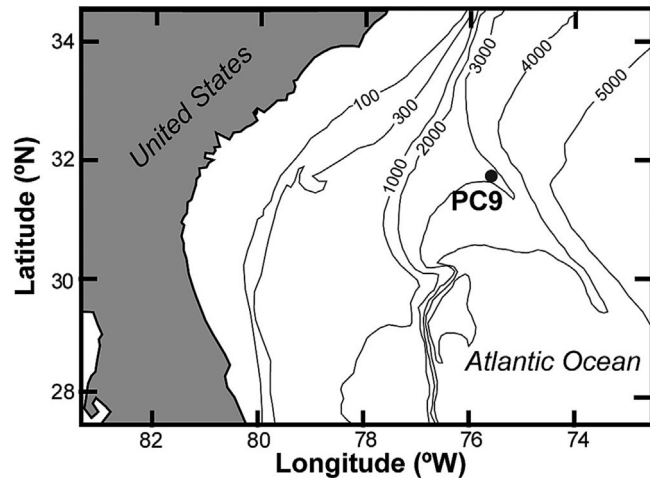


FIGURE A1 Map showing location and bathymetric setting of study area from which piston core PC9 was retrieved (contour lines in meters).

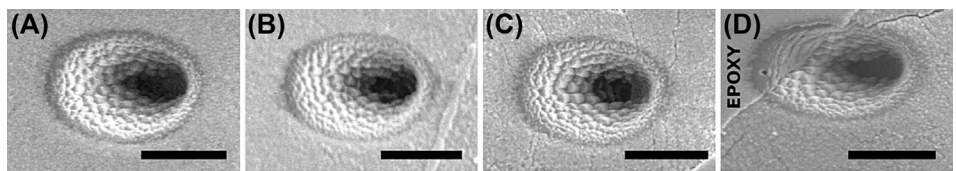


FIGURE A2 SE SEM images of SIMS $\delta^{13}\text{C}$ analysis pits for (A) UWC-3 standard, and shell analysis pits classified as (B) 1 (good), (C) 2 (questionable), and (D) 3 (irregular). Note the abnormal void/shape at the bottom of the pit in (C) and small cross-cutting cracks. The pit in (D) includes epoxy. All scale bars are 5 μm .

The scores determined from pit appearance were used to assign a final score to the analysis using the same scale from 1 to 3 and are noted in Table S1. In cases where both pit appearance and data quality were deemed acceptable (assigned a score of 1), the analysis was also deemed acceptable (final score = 1). If either the pit appearance or data quality were irregular (score = 3), the analysis was excluded (final score = 3). Several analyses had questionable or irregular pit appearances but acceptable data quality. For these analyses, the $\delta^{13}\text{C}$ values were evaluated relative to other measurements from the same shell. If the $\delta^{13}\text{C}$ value for the investigated datum was within the range of SIMS $\delta^{13}\text{C}$ values measured from the same shell, the point was given a final score of 1. If the $\delta^{13}\text{C}$ value was not within this range or no other acceptable measurements were obtained on the same shell, the datum was deemed questionable (final score = 2). Only data with a final score of 1 (~71% of all SIMS $\delta^{13}\text{C}$ measurements obtained for this

study) are plotted and discussed in the main text. Of the data that were excluded (final score of 2 or 3), 83% were removed due to poor data quality, ~8% were removed due to anomalous SIMS pit appearance, and ~9% were removed due to both poor data quality and SIMS pit appearance.

Although CH/C ratios are useful to detect secondary ions produced by a non-carbonate portion of the foraminifer, the ratios were not used for quality control purposes because they did not correlate with the measured $\delta^{13}\text{C}$ value. In the final dataset (measurements with a final score of 1), the background-corrected CH/C ratios of the *O. universa* chambers varied between 0.0015 and 0.030 and provide insight into the relative amounts of hydrogen-bearing components (e.g. organics, water, and hydrated phases) within the foraminifer calcite. These CH/C ratios are not calibrated by standards and should not be regarded as quantitative.